Citation: Clin Transl Sci (2020) 13, 520–528; doi:10.1111/cts.12734

ARTICLE

Prediction of Metabolite-to-Parent Drug Exposure: Derivation and Application of a Mechanistic Static Model

Ernesto Callegari[1], Manthena V.S. Varma[1] and R. Scott Obach[1,*]

In the development of new drugs, the prediction of metabolite-to-parent plasma exposure ratio in humans prior to administration in a clinical study has emerged as an important need. In this work, we derived a mechanistic static model based on first principles to estimate metabolite-to-parent plasma exposure ratio, considering the contribution of liver and gut metabolism and drug transport. Knowledge (or assumptions) of mechanisms of clearance and organs involved is required. Input parameters needed included intrinsic clearance, fraction of clearance to the metabolite of interest, various binding values, and, in some cases, active transport clearance. The principles are illustrated with four drugs that yield six metabolites, with one in which clearance is dependent on a pathway subject to genetic polymorphism. Overall, the approach yielded metabolite-to-parent ratios within about twofold of the actual values and, thus, can be valuable in decision making in the drug development process.

Study Highlights

WHAT IS THE CURRENT KNOWLEDGE ON THE TOPIC?
☑ Although the prediction of human drug pharmacokinetics from *in vitro* metabolism and transport data is well known, doing the same for metabolites has not been well established.

WHAT QUESTION DID THIS STUDY ADDRESS?
☑ In this study, the question addressed is whether metabolite-to-parent drug plasma exposure ratios in humans could be projected from *in vitro* data.

WHAT DOES THIS STUDY ADD TO OUR KNOWLEDGE?
☑ This study demonstrated that metabolite-to-parent drug plasma exposure ratios in humans could be projected from *in vitro* data. The equations needed for this have been derived from clearance concepts and delineate the input data required to accomplish this for other drugs and their metabolites.

HOW MIGHT THIS CHANGE CLINICAL PHARMACOLOGY OR TRANSLATIONAL SCIENCE?
☑ Application of this method prior to administration of new drug candidates to humans in phase I clinical trials will inform decisions regarding the need to characterize and measure potentially important drug metabolites. This will help in risk mitigation for important human drug metabolites. Appropriate measurement of metabolites in phase I clinical trials can help ensure seamless drug development timelines.

The projection of drug pharmacokinetics in humans from data gathered *in vitro* using human-derived reagents is a common activity in research aimed to design and develop new pharmacotherapies. Such data are used in decision making regarding which compounds to nominate from the discovery/design phase into the development phase in drug research. Success is frequently measured numerically (i.e., the fold-error between predicted vs. actual parameters, etc.), however, more important is whether the correct decisions were made regarding compound nomination into development, which can be measured in more of a qualitative manner (i.e., did the anticipated dosing regimen achieve target exposures, etc.).

Although the projection of drug pharmacokinetics is not without its challenges, there is also a need and desire to make projections of the clinical exposures to major circulating metabolites. Certainly, projecting exposures to drug metabolites that can contribute to pharmacological efficacy is important in attempting to understand the dosage regimen needed for pharmacodynamic effect. In addition, since the issuance of regulatory guidance[1–3] where metabolites with significant plasma exposure need to be evaluated for drug-drug interaction (DDI) potential, there has been an increased need to predict major circulating metabolites (i.e., which metabolites are of concern and how abundant they are relative to the parent drug). Reliable projection of metabolite exposures in humans, relative to parent drug, can be important when deciding whether investment needs to be made in the development of validated bioanalytical methods to measure the metabolite in human plasma in phase I clinical studies and whether animal species used in preclinical toxicology

[1]Pharmacokinetics, Pharmacodynamics, & Metabolism, Medicine Design, Pfizer Inc., Groton, Connecticut, USA. *Correspondence: R. Scott Obach (r.scott.obach@pfizer.com)
Received: September 30, 2019; accepted: November 27, 2019. doi:10.1111/cts.12734

evaluations demonstrate adequate exposure to the metabolite to underwrite safety risk assessments.

In previous work, attempts were made to test methods to project metabolite-to-parent drug ratios from *in vitro* metabolism and transport data using both static and dynamic physiologically-based pharmacokinetic models[4–8] and various assumptions and simplifications were applied. In this paper, the derivations of equations for a static mechanistic model that can be used to predict metabolite-to-parent drug ratios are presented. Final equations are built starting with basic clearance concepts[9] and the contribution of gut to metabolite formation has been added. The extended clearance concept[10] that also includes active transport as an important determinant in drug and metabolite disposition has been considered. This derivation shows the origins of all of the component terms and permits application of assumptions and shortcuts, when justified, in individual instances.

METHODS

Mechanistic model derivation

The objective is to predict the metabolite-to-parent drug exposure ratio, which is defined as the ratio of the area under the plasma concentration-time curve of metabolite-to-parent drug (AUC_M/AUC_D). (Note that definitions of all parameters described in this derivation are listed in **Table 1** for ease of reference.) The desired metabolite-to-parent drug ratio, AUC_M/AUC_D, is based on plasma values, as plasma is commonly used as the biological matrix for pharmacokinetic analysis in clinical studies. Because systemic plasma clearance (CL_{plasma}) is defined as the dose (D) divided by the plasma AUC, the derivation begins with:

$$\frac{AUC_M}{AUC_D} = \frac{D_M}{CL_{plasma,M}} \cdot \frac{CL_{plasma,D}}{D_D} \tag{1}$$

The subscripts D and M refer to the parent drug and metabolite, respectively. Thus, there are four parameters that need to be defined: the dose and plasma clearance values for the parent drug and the metabolite. Three of these parameters are relatively straightforward to define, however, the fourth, the "dose" of metabolite (D_M) is considerably more complex in its nature, because metabolite is not dosed *per se*. These parameters are explained below, based on the scheme shown in **Figure 1**.

Systemic clearance values for parent drug and metabolite

The systemic CL_{plasma} for parent drug and metabolite are estimated using Eq. 1a and 1b, respectively. The $CL_{plasma,D}$ and $CL_{plasma,M}$ terms refer to the systemic CL_{plasma} values for the parent drug and the metabolite and the systemic total blood clearance (CL_D) is further defined as the sum of hepatic blood clearance ($CL_{D(h)}$) and the nonhepatic blood clearance ($CL_{D(nh)}$). In cases where nonhepatic clearance is low ($CL_{D(nh)} \ll CL_{D(h)}$) then systemic CL_{plasma} is dependent on hepatic blood clearance and blood/plasma (B/P) ratio.

$$CL_{plasma,D} = \left(CL_{D(h)} + CL_{D(nh)}\right) \cdot (B/P)_D \tag{1a}$$

$$CL_{plasma,M} = \left(CL_{M(h)} + CL_{M(nh)}\right) \cdot (B/P)_M \tag{1b}$$

The estimation of nonhepatic blood clearance is dependent on the clearance mechanism, with renal clearance being the most common of nonhepatic mechanisms. Renal clearance can be estimated from scaling data from preclinical species or from *in vitro* studies ($CL_r = f_u$*GFR + CL_{sec}).[7,11–13] The hepatic blood clearance values are each defined using the well-stirred model for hepatic extraction[14] that includes hepatic blood flow (Q_h), fraction unbound in blood (f_u), and hepatic free intrinsic clearance (CL_{int}) for each:

$$CL_{D(h)} = \frac{Q_h \cdot f_{u,D} \cdot CL_{int,D}}{Q_h + f_{u,D} \cdot CL_{int,D}} \tag{2a}$$

$$CL_{M(h)} = \frac{Q_h \cdot f_{u,M} \cdot CL_{int,M}}{Q_h + f_{u,M} \cdot CL_{int,M}} \tag{2b}$$

The impact of the role of transporters in drug clearance has led to the application of the extended clearance model (Eq. 3a).[15–19] Considering the mechanistic components, the extended clearance concept defines the intrinsic hepatic clearance as an interplay of various processes, namely, $PS_{D,pd}$, which is the parent drug passive diffusion clearance; and $PS_{D,influx}$ and $PS_{D,efflux}$ represent the active (transporter-mediated) sinusoidal influx and basolateral efflux clearances, respectively. $CL_{int,D,met+bile}$ is the sum of the free metabolic and biliary intrinsic clearances (i.e., $CL_{int(D\rightarrow M)}$, $CL_{int(D\rightarrow other\ metabolites}$, and $CL_{int,D\rightarrow bile)}$).[20]

$$CL_{int,D} = \frac{\left(PS_{D,influx} + PS_{D,pd}\right) \cdot CL_{int,D,met+bile}}{\left(PS_{D,efflux} + PS_{D,pd} + CL_{int,D,met+bile}\right)} \tag{3a}$$

The total hepatic clearance ($CL_{D(h)}$) can be calculated by assuming well-stirred conditions using Eq. 3b[14,21]

$$CL_{D(h)} = \frac{Q_h \cdot f_{u,D} \cdot \left(PS_{D,influx} + PS_{D,pd}\right) \cdot CL_{int,D,met+bile}}{Q_h \cdot \left(PS_{D,efflux} + PS_{D,pd} + CL_{int,D,met+bile}\right) + f_{u,D} \cdot \left(PS_{D,influx} + PS_{D,pd}\right) \cdot CL_{int,D,met+bile}} \tag{3b}$$

Corresponding relationships will exist for the metabolite as well, with slightly different underlying terms (i.e., $CL_{int,M,met+bile}$ has just two terms: $CL_{int(M\rightarrow other\ metabolites}$, and $CL_{int,M\rightarrow bile)}$).

$$CL_{int,M} = \frac{\left(PS_{M,influx} + PS_{M,pd}\right) \cdot CL_{int,M,met+bile}}{\left(PS_{M,efflux} + PS_{M,pd}\right) + CL_{int,M,met+bile}} \tag{3c}$$

$$CL_{M(h)} = \frac{Q_h \cdot f_{u,M} \cdot \left(PS_{M,influx} + PS_{M,pd}\right) \cdot CL_{int,M,met+bile}}{Q_h \cdot \left(PS_{M,efflux} + PS_{M,pd} + CL_{int,M,met+bile}\right) + f_{u,M} \cdot \left(PS_{M,influx} + PS_{M,pd}\right) \cdot CL_{int,M,met+bile}} \tag{3d}$$

Table 1 Index of parameters used in the equations

Parameter	Definition
AUC_M	Area under the plasma concentration vs. time curve for the metabolite
AUC_D	Area under the plasma concentration vs. time curve for the parent drug
$(B/P)_D$	Blood to plasma ratio for the parent drug
$(B/P)_M$	Blood to plasma ratio for the metabolite
CL_D	Systemic blood clearance of the parent drug
$CL_{D(h)}$	Hepatic blood clearance of the parent drug
$CL_{D(nh)}$	Nonhepatic blood clearance of the parent drug
$CL_{int,D}$	Free intrinsic clearance of the parent drug in the liver
$CL_{int(D\rightarrow bile)}$	Free intrinsic clearance of biliary secretion of parent drug
$CL_{int(D\rightarrow liver)}$	Free intrinsic clearance of drug entering the liver
$CL_{int(D\rightarrow M)}$	Free intrinsic clearance of parent drug conversion to the metabolite in the liver
$CL_{int,D,met+bile}$	Sum of free intrinsic clearance of parent drug by metabolism and biliary secretion
$CL_{int(D\rightarrow other\ metabolites)}$	Free intrinsic clearance of parent drug conversion to other metabolites in the liver
$CL_{int,g(D)}$	Free intrinsic clearance of parent drug in the gut
$CL_{int,g(D\rightarrow M)}$	Free intrinsic clearance of parent drug conversion to the metabolite in the gut
$CL_{int,g(D\rightarrow other\ metabolites)}$	Free intrinsic clearance of parent drug conversion to other metabolites in the gut
$CL_{int,g(M\rightarrow blood)}$	Free intrinsic clearance of metabolite entry from enterocytes into the portal vein blood
$CL_{int,g(M\rightarrow lumen)}$	Free intrinsic clearance of metabolite efflux from enterocytes into the gut lumen
$CL_{int,g(M\rightarrow other\ metabolites)}$	Free intrinsic clearance of the metabolite to other metabolites in the gut
$CL_{int(M\rightarrow bile)}$	Free intrinsic clearance of biliary secretion of the metabolite
$CL_{int(M\rightarrow blood)}$	Free intrinsic clearance of secretion of the metabolite from the liver to the blood
$CL_{int(M\rightarrow liver)}$	Free intrinsic clearance of metabolite entering the liver
$CL_{int,M,met+bile}$	Sum of free intrinsic clearance of metabolite by further metabolism and biliary secretion
$CL_{int(M\rightarrow other\ metabolites)}$	Free intrinsic clearance of the metabolite to other metabolites in the liver
$CL_{int,M}$	Free intrinsic clearance of the metabolite in the liver
CL_M	Systemic blood clearance of the metabolite
$CL_{M(h)}$	Hepatic blood clearance of the metabolite
$CL_{M(nh)}$	Nonhepatic blood clearance of the metabolite
$CL_{plasma,D}$	Systemic plasma clearance of the parent drug
$CL_{plasma,M}$	Systemic plasma clearance of the metabolite
CL_r	Renal clearance
$CL_{sec,D}$	Renal secretory clearance of the parent drug
$CL_{sec,M}$	Renal secretory clearance of the metabolite
D	Actual dose of the parent drug administered
D_D	Amount of parent drug that gets to the systemic circulation after oral administration
D_M	Amount of the metabolite to which the body is exposed systemically
$D_{M,gut,first\ pass}$	Amount of metabolite generated by the intestine during absorption of oral administration of parent drug
$D_{M,hepatic,first\ pass}$	Amount of metabolite generated by the liver during first pass after oral administration of parent drug
$D_{M,hepatic,systemic}$	Amount of metabolite generated by the liver from systemically available parent drug
F_a	Fraction of the parent drug that is absorbed following oral administration
F_g	Fraction of the parent drug that evades extraction by the intestine during first pass following oral administration
F_h	Fraction of the parent drug that is evades extraction by the liver during first pass following oral administration
$F_{M(g)}$	Fraction of the metabolite generated in the gut that enters the portal vein
$f_{m(g)}$	Fraction of the gut metabolism of the parent drug that results in the generation of the metabolite
$F_{M(h)}$	Fraction of the metabolite generated in the liver that enters the circulation
$f_{m(h)}$	Fraction of the hepatic clearance of the parent drug that results in the generation of the metabolite
$f_{u,D}$	Fraction of the parent drug unbound in blood
$f_{u,M}$	Fraction of the metabolite unbound in blood
GFR	Glomerular filtration rate
$PS_{D,efflux}$	Parent drug clearance by active efflux from the cell
$PS_{D,influx}$	Parent drug clearance by active uptake into the cell
$PS_{D,pd}$	Parent drug clearance by passive diffusion across the cell membrane
$PS_{M,efflux}$	Metabolite clearance by active efflux from the cell
$PS_{M,influx}$	Metabolite clearance by active uptake into the cell
$PS_{M,pd}$	Metabolite clearance by passive diffusion across the cell membrane
Q_h	Hepatic blood flow

The interplay of the four parameters of Eq. 3a determines drug hepatic clearance and defines the rate-determining step of drug clearance. Equation 3b can be reduced to Eq. 2a (and 2b for metabolite) when "rapid-equilibrium" is assumed between liver and blood compartments; that is, when the compound is not subjected to active transport mechanisms across the basolateral membrane, and the PS_{pd} is significantly higher than $CL_{int,met+bile}$.

Equation 3b and 3d can also be simplified to Eq. 3e and 3f, where the systemic clearance uptake is determined for compounds with relatively slower basolateral (active and passive) efflux (i.e., $PS_{efflux} + PS_{pd} \ll CL_{int,met+bile}$ (e.g., statins and sartans)).[17,18,21]

$$CL_{D(h)} = \frac{Q_h \cdot f_{u,D} \cdot (PS_{D,influx} + PS_{D,pd})}{Q_h + f_{u,D} \cdot (PS_{D,influx} + PS_{D,pd})} \quad (3e)$$

$$CL_{M(h)} = \frac{Q_h \cdot f_{u,M} \cdot (PS_{M,influx} + PS_{M,pd})}{Q_h + f_{u,M} \cdot (PS_{M,influx} + PS_{M,pd})} \quad (3f)$$

Dose of the parent drug

The term D_D in Eq. 1 refers not to the nominal dose administered, but to the amount of parent drug that gets to the systemic circulation after oral administration (i.e., the bioavailable dose). If the parent drug is administered parenterally, then the dose term used in the equation is the actual dose

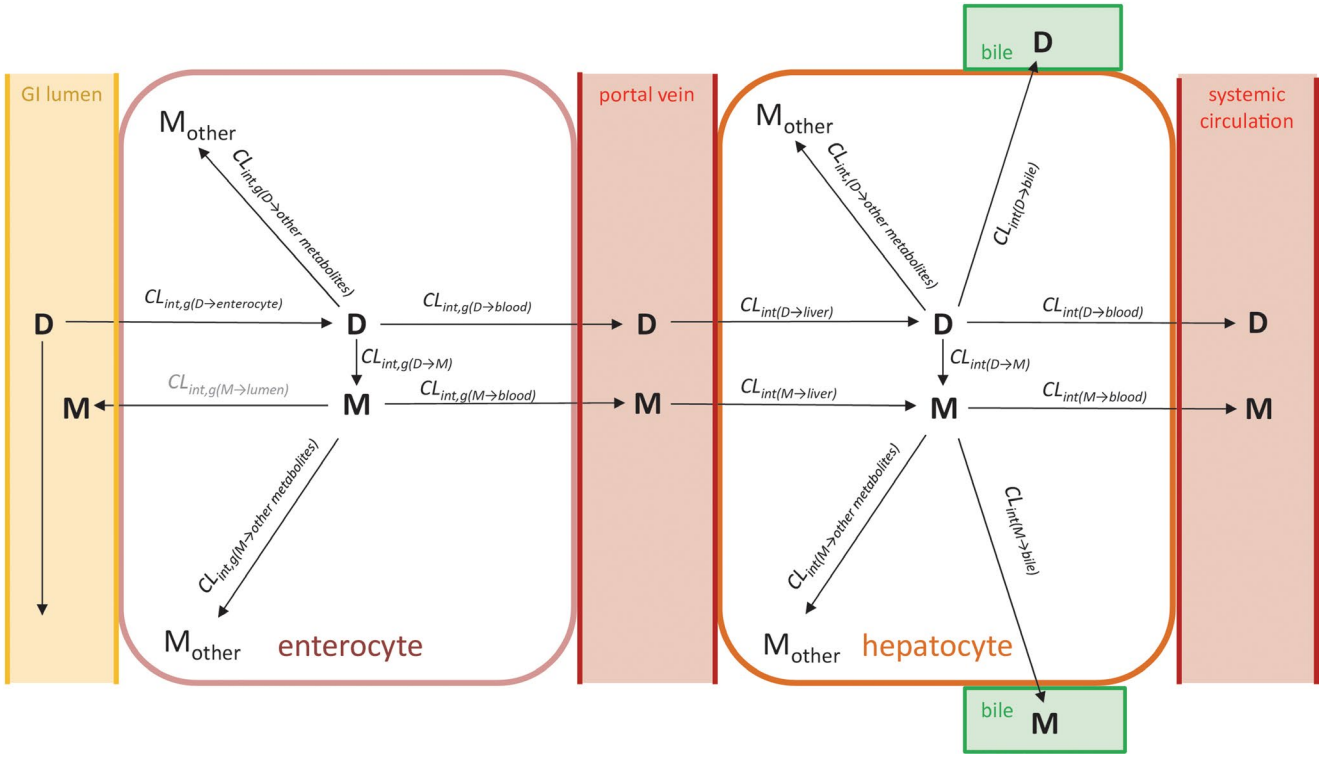

Figure 1 Model schematic showing the dispositional processes for parent drug (D) and metabolite (M). CL_{int}, intrinsic clearance.

administered. However, if the dose is administered orally, then the term needs to be corrected for any limits on absorption (F_a) as well as any first-pass extraction by the intestine (F_g) and liver (F_h):

$$D_D = D \cdot F_a \cdot F_g \cdot F_h \quad (4)$$

where D is the actual dose administered in molar units. In cases where clinical AUC ratios are obtained from exposure data in gram units (e.g., ng·hour/mL), predicted metabolite-to-parent ratios need to be corrected for differences in molecular weight between parent and metabolite.

Dose of the metabolite

The term D_M (or "dose" of the metabolite) is by far the most complicated one to derive. Unlike the parent drug, the metabolite is not dosed *per se*, but is generated within the body from the parent drug. In this treatment, the metabolite can be potentially generated from three sources following oral administration of the parent drug: (i) generated systemically by the liver, (ii) generated by the liver during first-pass extraction of the parent drug, and (iii) generated by the intestine during first-pass (Eq. 5). In cases where the enzyme forming the metabolite is not present in the enterocytes, then the intestinal first-pass contribution to D_M is assumed to be negligible (i.e., $D_{M,gut,first\ pass} = 0$). Similarly, if the parent drug is administered intravenously, only metabolite generated systemically by the liver is considered in estimating D_M.

$$D_M = D_{M,hepatic,systemic} + D_{M,hepatic,first\ pass} + D_{M,gut,first\ pass} \quad (5)$$

The estimate of metabolite generated in the liver from the systemically available parent drug ($D_{M,hepatic,systemic}$) is defined in Eq. 6:

$$D_{M,hepatic,systemic} = D_D \cdot \frac{CL_{D(h)}}{CL_D} \cdot f_{m(h)} \cdot F_{M(h)} \quad (6)$$

The metabolite that can be generated in the liver is restricted to the amount of the parent drug to which the liver is exposed systemically, which is defined above as D_D (from Eq. 4). The ratio $CL_{D(h)}/CL_D$ is the fractional contribution of the liver to the total blood clearance of the parent drug. The amount of the metabolite generated in the liver will be limited by the amount of liver clearance ($CL_{D(h))}$) relative to total clearance (CL_D), which can also include renal or extrahepatic clearance of the parent drug that could divert the parent drug from conversion to metabolite. The term $f_{m(h)}$ is the fraction of hepatic clearance of the parent drug that yields the metabolite of interest. The liver uptake and efflux transporters impact the rate of systemic clearance of the parent drug and are incorporated into the estimation of $CL_{D(h))}$. Thus, assuming steady state and these transporters are not considered hepatic clearance mechanisms, the $f_{m(h)}$ is represented by a ratio of intrinsic clearance terms:

$$f_{m(h)} = \frac{CL_{int(D→M)}}{CL_{int(D→M)} + CL_{int(D→other\ metabolites)} + CL_{int(D→bile)}} \quad (7)$$

wherein $CL_{int(D→M)}$ is the free intrinsic clearance for the parent drug conversion to the metabolite of interest, $CL_{int(D→other\ metabolites)}$ is the free intrinsic clearance for

conversion of the parent drug to other metabolites, and $CL_{int(D\rightarrow bile)}$ is the free intrinsic clearance of biliary secretion of the parent drug. If there is no biliary clearance of parent drug, then the $f_{m(h)}$ term is the fraction of total hepatic metabolism comprised by the pathway of interest.

The term $F_{M(h)}$ represents an "availability" term (i.e., the availability of the metabolite), once formed within the liver, to escape the liver and enter the systemic circulation. Once generated inside the hepatocyte, the metabolite can undergo three fates: further sequential metabolism, secretion into the bile, or secretion into the blood. These can be represented by a ratio of intrinsic clearance terms $CL_{int(M\rightarrow other\ metabolites)}$, $CL_{int(M\rightarrow bile)}$, and $CL_{int(M\rightarrow blood)}$, respectively:

$$F_{M(h)} = \frac{CL_{int(M\rightarrow blood)}}{CL_{int(M\rightarrow blood)} + CL_{int(M\rightarrow other\ metabolites)} + CL_{int(M\rightarrow bile)}} \quad (8a)$$

Alternately, for highly permeable compounds where egress through the membrane is not limiting, the term $F_{M(h)}$ can be described by a simpler equation:

$$F_{M(h)} = \frac{Q_h}{Q_h + f_{u,M} \cdot CL_{int,M,met+bile}} \quad (8b)$$

wherein the availability of metabolite generated in the liver is driven by competition between further clearance in the liver (metabolism and/or biliary secretion) and liver blood flow carrying the metabolite away from the liver and into the systemic circulation.

The metabolite generated during first pass hepatic extraction is $D_{M,hepatic,first\ pass}$, and is outlined in Eq. 9. The equation is similar to Eq. 6, except that the dose term is different and no consideration of extrahepatic clearance is needed.

$$D_{M,hepatic,first\ pass} = D \cdot F_a \cdot F_g \cdot (1 - F_h) \cdot f_{m(h)} \cdot F_{M(h)} \quad (9)$$

The amount of parent drug presented to the liver for first-pass is defined as $D{\cdot}F_a{\cdot}F_g$ and the amount of metabolite formed during first-pass and released to the systemic circulation is modified by the term: $(1\text{-}F_h){\cdot}f_{m(h)}{\cdot}F_{M(h)}$.

Finally, some conversion of the parent drug to the metabolite can occur in the intestine, particularly for substrates of drug metabolizing enzymes, such as cytochrome P450 (CYP)3A4. This pool of metabolite is generated in the gut, enters the portal vein, and is then subject to hepatic extraction by the liver before entering systemic circulation. The expression for this is:

$$D_{M,gut,first\ pass} = D \cdot F_a \cdot (1 - F_g) \cdot f_{m(g)} \cdot F_{M(g)} \cdot \left(1 - \frac{CL_{M(h)}}{Q_h}\right) \quad (10)$$

The amount of parent drug that enters the enterocytes is defined as $D{\cdot}F_a$ and the portion of this dose that is converted to metabolite in the intestine enterocytes and released into the portal vein is defined as $(1\text{-}F_g){\cdot}f_{m(g)}{\cdot}F_{M(g)}$. The last term $(1\text{-}CL_{M(h)}/Q_h)$ represents the hepatic extraction of the metabolite released into the portal vein before it can be available systemically. The term $f_{m(g)}$ is the fraction of gut clearance of the parent drug that yields the metabolite. In the gut, the only clearance mechanism assumed is metabolism, therefore, $f_{m(g)}$ is defined as:

$$f_{m(g)} = \frac{CL_{int,g(D\rightarrow M)}}{CL_{int,g(D\rightarrow M)} + CL_{int,g(D\rightarrow other\ metabolites)}} \quad (11)$$

$CL_{int,g(D\rightarrow M)}$ is the free intrinsic clearance of the parent drug to the metabolite in enterocytes and $CL_{int,g(D\rightarrow other\ metabolites)}$ corresponds to the metabolism of the parent drug to other metabolites in the gut. Unlike the corresponding term for the liver, there is no "out" or "bile" CL_{int} terms because they are already accounted for in the F_a term in Eq. 10. In the gut, it is assumed that F_a represents the net absorption, which takes into account the efflux back into the gastrointestinal lumen. Thus, metabolism is the only clearance mechanism contributing to $f_{m(g)}$.

The term $F_{M(g)}$ is the fraction of the metabolite generated in the intestine that gets into the portal vein.

$$F_{M(g)} = \frac{CL_{int,g(M\rightarrow blood)}}{CL_{int,g(M\rightarrow blood)} + CL_{int,g(M\rightarrow other\ metabolites)} + CL_{int,g(M\rightarrow lumen)}} \quad (12)$$

Once formed in the enterocyte, the metabolite can undergo three possible fates. It can enter the portal vein ($CL_{int,g(M\rightarrow blood)}$), be further metabolized ($CL_{int,g(M\rightarrow other\ metabolites)}$), or be secreted into the gut ($CL_{int,g(M\rightarrow lumen)}$).

In this estimate of D_M, it is assumed that the metabolite is only formed in the liver, from systemic and first-pass extraction, and in the gut, from first-pass extraction, whereas metabolite formed in other organs of clearance is not considered. Absorption of the metabolite from the gut, by reabsorption of secreted metabolite, or enterohepatic circulation of metabolite, or hydrolysis of metabolite glucuronides in the gastrointestinal tract is not included. There may be specific cases in which these mechanisms need to be accounted for in estimates of D_M, and they offer a level of further complexity not pursued in this derivation.

Experimental *in vitro* and human pharmacokinetic data

All *in vitro* metabolism and binding data for midazolam, 1′-hydroxymidazolam, 4-hydroxymidazolam, imipramine, desipramine, (R)-4-((4-(((4-((tetrahydrofuran-3-yl)oxy)benzo[d]isoxazol-3-yl)oxy)methyl)piperidin-1-yl)methyl)tetrahydro-2H-pyran-4-ol (TBPT), an experimental serotonin receptor drug), TBPT-M1, and TBPT-M2 were previously measured.[5,6,8] *In vitro* metabolism, transport, and binding data for losartan and carboxylosartan were previously reported.[7] The clinical metabolite-to-parent drug ratios were from reports in the literature and were summarized in previous reports.[5–8]

RESULTS

Derivation of a mechanistic static model for projection of plasma metabolite-to-parent exposure ratios was successfully accomplished. The model was tested on six previously described examples of metabolite/parent pairs. These represent P450, UGT, and active transport clearance processes and were selected because the needed *in vitro* input data were already available and human exposure values for parent and metabolite are

known. Input data and parameters are listed in **Table 2**. A summary of the projected metabolite-to-parent exposure ratios are listed in **Table 3**. The model-predicted values are generally within twofold of the observed plasma metabolite-to-parent ratios (**Figure 2**). Hydroxymidazolam metabolites are predicted to have exposures that are lower than the parent midazolam; and these predictions are in agreement with the observed values.[22–26] For 1′-hydroxymidazolam, the predicted ratio is 0.67 and reported values range between 0.3 and 0.6, and for 4-hydroxymidazolam, the predicted ratio was 0.05, whereas reported measured values were 0.06 and 0.08. For both midazolam metabolites, ~ 40% of the metabolite formation was predicted to be due to metabolism in the gut. In CYP2D6 extensive metabolizers, desipramine exposure is predicted to be about 84% that of the parent imipramine, which is similar to the clinical exposure. However, in poor metabolizer (MP) subjects, the ratio is predicted to be considerably greater than unity (11-fold), which is higher than the reported range (~ 3 to 7).[27–33] Nevertheless, the predictions via this approach offer a similar picture of metabolite-to-parent exposure relationships in these two populations.

TBPT offers an interesting example where one metabolite is much greater than parent and one much less. *In vitro*, TBPT is metabolized by P450 enzymes to yield an N-dealkylated product (M1), a cyclized product (M2), as well as two other hydroxylated metabolites.[34] For TBPT, the very high metabolite-to-parent ratio for M2 in plasma is reasonably approached (projected at 23 vs. actual of 58), and the corresponding low ratio for the other metabolite is also well predicted (0.17 projected vs. 0.12 actual).

On the other hand, losartan and carboxylosartan involve transporter-mediated disposition, which determine their clearance and intracellular concentrations within the hepatocyte. Here, the measured carboxylosartan-to-losartan exposure ratios range from 2.6 to 7.5,[35–40] whereas the predicted value is greater at 14. Because losartan is a substrate for active uptake and efflux, the fraction of losartan clearance resulting in carboxylosartan ($f_{m(h)}$) was estimated using Eq. 7 and systemic availability of carboxylosartan from the liver following its generation ($F_{m(h)}$) was estimated using Eq. 8a. For carboxylosartan,

Table 2 Summary input parameters used for estimation of metabolite-to-parent drug ratios for midazolam, imipramine, losartan, TBPT, and their metabolites

Drug	Midazolam[6]		Imipramine[5]		TBPT[8]		Losartan[7]
Metabolite	**1′-Hydroxy**	**4-Hydroxy**	**Desipramine (CYP2D6 EM)**	**Desipramine (CYP2D6 PM)**	**M1**	**M2**	**Carboxylosartan**
Clearance terms (scaled to mL/minutes/kg)							
CL_D	9.7		9.4		7.9		12.8[c]
CL_M	11.9	11.2	6.4	1.0	11.0	0.4	0.64[d]
$CL_{int(D\rightarrow M)}$	344	20.6	8.2	8.2	10.8	11.5	6.8
$CL_{int,g(D\rightarrow M)}$	2.8	0.17	–	–	0.2	0.3	–
$CL_{int(M\rightarrow other\ metabolites)}$	184	183	19.8	2.2	29	92	0
Dose terms (in μmoles)							
D	6.1		267		35		108
F_a	1		1		1		1
F_g	0.57		1		0.94		1
F_h	0.54		0.55		0.62		0.46
D_D	1.8		147		5.8		50
$D_{M,hepatic,systemic}$	0.74	0.05	55	115	3.9	8.2	16
$D_{M,hepatic,first\ pass}$	0.65	0.05	45	94	2.4	5.0	21
$D_{M,gut,first\ pass}$	1.0	0.07	0	0	0.3	1.2	0
D_M	2.4	0.17	100	209	6.6	14	37
Measured binding terms							
$f_{u,D}$	0.03		0.26		0.38		0.028
$(B/P)_D$	0.6		1.02		0.86		0.53
$f_{u,M}$	0.15	0.13	0.21		0.64	0.0025	0.0024
$(B/P)_M$	1	1	1.16		0.88	0.53	0.58
Calculated metabolism and availability terms							
$f_{m(h)}$[a]	0.93	0.06	0.44	0.8	0.41	0.41	0.37
$f_{m(g)}$	0.93	0.06	0	0	0.30	0.58	0
$F_{M(h)}$[b]	0.43	0.47	0.85	0.98	0.47	0.98	1
$F_{M(g)}$	1	1	N/A	N/A	1	1	n/a

EM, extensive metabolizer; N/A, not applicable; PM, poor metabolizer; TBPT, (R)-4-((4-(((4-((tetrahydrofuran-3-yl)oxy)benzo[d]isoxazol-3-yl)oxy)methyl) piperidin-1-yl)methyl)tetrahydro-2H-pyran-4-ol.

[a]$f_{m(h)}$ calculated using Eq. 7 and data from references. [b]$F_{M(h)}$ for midazolam, imipramine, and TBPT assumed $CL_{int(M\rightarrow blood)} \gg Q_h$ (Eq. 8b). $F_{M(h)}$ for losartan used Eq. 8a. [c]CL_D for losartan = $CL_{D(h)} + CL_{D(nh)}$, $CL_{D(h)}$ = 11.1 and $CL_{D(nh)}$ = 1.7. [d]CL_M for carboxylosartan = $CL_{M(h)} + CL_{M(nh)}$, $CL_{M(h)}$ = 0, $CL_{M(nh)}$ = 0.64.[5–8]

Table 3 Projections of metabolite-to-parent drug plasma AUC ratios for six metabolites and four drugs following oral administration of the drugs

Parent drug	Metabolite	Parent to metabolite(s)	Metabolite clearance	Predicted M/P[a]	Actual M/P	References
Midazolam	1′-hydroxymidazolam	CYP3A4/5	UGT	0.67	0.3–0.6	22–26
	4-hydroxymidazolam			0.05	0.08, 0.06	
Imipramine	Desipramine (EM)	CYP2C19	CYP2D6	0.84	0.48–1.1	27–34
	Desipramine (PM)			11	2.8–6.8	
TBPT	M1	CYP3A4	CYP	0.17	0.12	35
	M2			23	58	
Losartan	Carboxylosartan	CYP2C9	Transport	14	2.6–7.5	36–41

AUC, area under the curve; EM, extensive metabolizer; M/P, metabolite/parent; PM, poor metabolizer; TBPT, (R)-4-((4-(((4-((tetrahydrofuran-3-yl)oxy)benzo[d]isoxazol-3-yl)oxy)methyl)piperidin-1-yl)methyl)tetrahydro-2H-pyran-4-ol.
[a]Molecular weight of parent and metabolite incorporated in M/P.

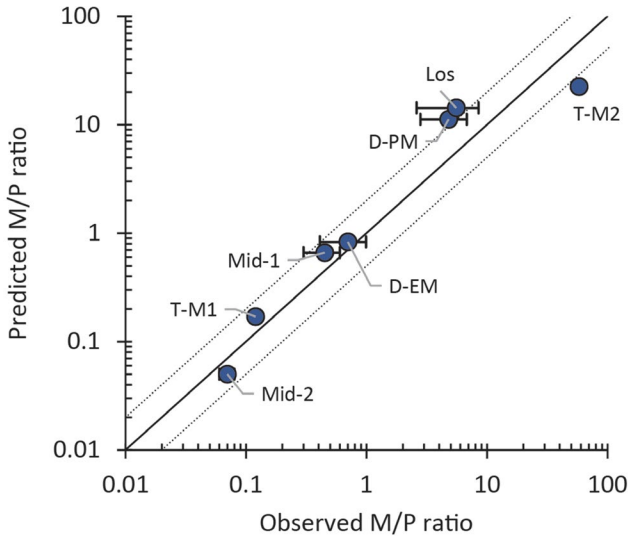

Figure 2 Predicted vs. observed metabolite-to-parent drug plasma area under the curve ratios for six metabolites and four drugs following oral administration of the drugs. Solid and dotted lines represent unity and twofold deviation, respectively. For clinical data, when more than one study was identified that contained metabolite and parent drug exposure data, the horizontal lines represent the highest and lowest values reported and the plotted point is the midpoint of these two values. D-EM, desipramine in extensive metabolizers; D-PM, desipramine in poor metabolizers; Los, carboxylosartan; Mid-1, 1′-hydroxy midazolam; Mid-2, 4′-hydroxy midazolam; T-M1, TBPT M1; T-M2, TBPT M2.

the $F_{m(h)}$ was unchanged ($F_{m(h)}$ = unity), whereas the updated losartan $f_{m(h)}$ was 0.37, which was greater than that previously estimated ($f_{m(h)}$ = 0.076).[7] Example worksheets used to make estimates of metabolite/parent (M/P) ratios are included as a **supplement**.

DISCUSSION

Overall, the equations derived in this report for the projection of metabolite-to-parent exposure ratios in human plasma were successfully used. The types of input data needed for these predictions are routinely gathered for drug candidates during early preclinical research in support of human dosing, however, extra effort would be needed to gather the similar data sets for metabolites of interest because such data are not routinely gathered. The promise of this approach can be used to justify gathering such data for metabolites in the preclinical stages of drug development. It is important to note that no matter how sound the theoretical basis is for this prediction method, successful implementation is highly dependent on the fidelity of the *in vitro* reagents, experimental methods used to generate the input data, and confidence in necessary scaling factors. *In vitro* intrinsic clearance, metabolite profiles, plasma and blood binding, and active transport flux values all have their own scaling factors. For example, measurement of *in vitro* plasma protein binding is generally more facile and reliable than measurements of *in vitro* metabolic intrinsic clearance or transport flux values. Errors and/or lack of physiological scaling for some methods could impart some error into predictions of metabolite-to-parent ratios. In some cases, some errors may cancel each other out because it is a M/P ratio that is being sought. Many of the measurements needed for this approach requires availability of metabolite standards. However, because these experiments are *in vitro*, only very small amounts are needed (< 1 mg) and these materials can be accessed using modern biosynthetic methods.[42]

The projection of metabolite-to-parent ratios for 1′-hydroxymidazolam and 4-hydroxymidazolam was successful (**Table 3**). Midazolam and its metabolites are highly membrane permeable, not shown to be subject to active transport, and their generation and disposition are mediated by metabolism (CYP and UGT enzymes).[43,44] Because these metabolites are known to be generated not only in the liver, but the intestine as well, midazolam offered a good test to determine whether metabolite-to-parent ratios can be estimated when a substantial portion of metabolite is generated by the intestine. From this example, it can be concluded that the method can work for metabolites generated by intestinal CYP3A4.

The example of imipramine and its desmethyl metabolite, desipramine, offered an interesting case where populations of CYP2D6 extensive and PMs show different metabolite-to-parent ratios because of the involvement of CYP2D6 as a major enzyme in desipramine clearance. The prediction method showed that exposures to imipramine and desipramine would be similar to each other in extensive metabolizers, but the metabolite-to-parent ratio would be high in PMs). This is consistent with the knowledge that desipramine is generated

from imipramine by enzymes other than CYP2D6 (mostly CYP2C19)[45] but that desipramine is cleared by CYP2D6.[46] The metabolite-to-parent ratio was overpredicted for PM subjects (predicted 11 vs. actual values of 2.6–6.8),[27–34] but if considered prospectively as if imipramine were a new drug candidate, it would be predicted that the metabolite would be quantitatively very important in PM subjects.

In the case of TBPT, one metabolite (M1) is much lower than parent and the other (M2) much higher and these cases were both well predicted. The M1 metabolite of TBPT results from an N-dealkylation reaction wherein ~ 25% of the molecule is lost. Thus, to estimate the AUC_M/AUC_P for M1 measured in mass per volume units, the AUC_M/AUC_P value estimated from *in vitro* data needed to be corrected for the molecular weight difference between TBPT and M1. For M2, the B/P ratios differ markedly between parent and metabolite (0.86 and 0.53, respectively), thus the AUC_M/AUC_P that was calculated had to be corrected for B/P ratio differences to better reflect the measured plasma ratio. In most instances, drugs and their metabolites may not exhibit great differences in B/P ratio or molecular weight, but the example of TBPT serves as a reminder that such factors should not be ignored when attempting to predict plasma metabolite-to-parent exposure ratios.

Among the drugs used to test metabolite prediction methods, losartan offers unique challenges because active transport is an important determinant in exposure to parent and metabolite. Thus, extended clearance concepts are needed for prediction. The predicted metabolite-to-parent ratio was 14 whereas reported clinical ratios range from 2.6 to 7.5.[36–41] It is possible that a clearance pathway for carboxylosartan is unaccounted for, or that the rates of clearance for known pathways are underestimated from *in vitro* data. It is noteworthy that following an intravenous dose of carboxylosartan to humans only half of the systemic clearance could be accounted for by renal clearance, suggesting an alternate mechanism for carboxylosartan clearance that was not accounted for in this analysis.[47] Furthermore, in a study with radiolabeled losartan administered intravenously, approximately half of the dose was excreted in feces (Cozaar Package Insert).[48] The source of this material was not accounted for but could be related to further biliary clearance of carboxylosartan or excretion of downstream metabolites. Thus, it is possible that carboxylosartan has unknown hepatic clearance mechanisms that could be important but not able to be included in calculations for estimating M/P exposure ratios. Although losartan is the only well-established transporter substrate in this data set, the predictions are reasonably similar to the observed values (i.e., M/P ratio is well over unity). As drug transporters are an area of active research, it is expected that improvements in the methods of their study will enable better estimates of transport parameters and improve projections of metabolite-to-parent ratios.

Overall, the concepts and derived equations predicted the M/P ratios for the six M/P examples within about twofold of measured values (**Figure 2**). Assumptions needed for this approach include those required when applying any *in vitro* data to understanding *in vivo* drug metabolism and pharmacokinetics. In addition, assumptions regarding the clearance mechanisms and organs for the parent drug and metabolites of interest must be taken. Because metabolites have the potential to contribute to efficacy, toxicity, and DDIs, there is an increased focus on identification of metabolites and assessing exposures in drug research and preclinical development in advance of clinical studies. Guidance documents from government drug regulatory authorities have been issued regarding drug metabolites.[1–3] These call for comparison of metabolite exposure levels in animals used in toxicological assessments vs. humans, as well as evaluation of metabolites as potential inhibitors of drug metabolizing enzymes and transporters, which can result in pharmacokinetic DDIs. Thresholds for when metabolites are important are based on quantitative relative human exposure data. Thus, decisions are needed regarding whether to make early investments in the synthesis of bulk quantities of specific drug metabolites before human dosing commences. When synthesized, the materials can be used in the development and validation of bioanalytical methods as well as tests as inhibitors of important drug metabolizing enzymes and transporters. The methods described in this paper can be used to make decisions earlier in the drug development process regarding which metabolites may be quantitatively important in humans. These metabolites can be proactively evaluated to help avoid delays in drug development later in the process. It should be noted that for the aforementioned decision making, the prediction of general "zones" is all that is needed rather than numerically accurate estimations—will the metabolite be in great excess relative to the parent drug, nominally greater, nominally lower, or far lower? The approach described can certainly serve that purpose. Finally, it is important to note that each new drug will possess its own array of properties that can yield different challenges to this endeavor. This is especially true for clearance mechanisms, as these can be widely varied, and when different from the examples described, some different experiments and input values may be necessary.

In conclusion, the prediction of human drug metabolite exposures for new drug candidates is not without its challenges, with assumptions required regarding mechanisms of clearance *in vivo* as well as limitations on the fidelity, performance, and scalability of various human-derived *in vitro* systems. Nevertheless, the findings reported here offer promise that this can be done, if not with quantitative accuracy, at least with enough accuracy for good decision making regarding the extent to which drug metabolites should be proactively studied and characterized ahead of dosing the parent drug in human trials. Ongoing endeavors include expanding the number of drugs evaluated to cover other clearance mechanisms as well as attempts to utilize physiologically-based pharmacokinetic modeling to predict metabolite exposure.

Supporting Information. Supplementary information accompanies this paper on the *Clinical and Translational Science* website (www.cts-journal.com).

Supplemental Material. Spreadsheet for Estimation of Metabolite/Parent Ratio.

Acknowledgments. The authors wish to acknowledge their managers, Drs. Dennis Scott, A. David Rodrigues, and Susanna Tse, for supporting this work. They would also like to acknowledge Dr. Stephen Hall of Eli Lilly for helpful discussions of this area of science.

Funding. No funding was received for this work.

Conflict of Interest. The authors are employees of Pfizer Inc.

Author Contributions. All authors wrote the manuscript, designed the research, performed the research, and analyzed the data.

1. US Food and Drug Administration (FDA). In Vitro Metabolism- and Transporter-Mediated Drug-Drug Interaction Studies Guidance for Industry (2017). <https://www.fda.gov/regulatory-information/search-fda-guidance-documents/vitro-metabolism-and-transporter-mediated-drug-drug-interaction-studies-guidance-industry>.
2. US Food and Drug Administration (FDA). Safety Testing of Drug Metabolites (2016). <https://www.fda.gov/regulatory-information/search-fda-guidance-documents/safety-testing-drug-metabolites>.
3. European Medicines Agency (EMA). Guideline on the investigation of drug interactions. <https://www.ema.europa.eu/en/investigation-drug-interactions>.
4. Lutz, J.D. & Isoherranen, N. Prediction of relative in vivo metabolite exposure from in vitro data using two model drugs: dextromethorphan and omeprazole. *Drug Metab. Dispos.* **40**, 159–168 (2012).
5. Nguyen, H.Q., Callegari, E. & Obach, R.S. The use of in vitro data and physiologically-based pharmacokinetic modeling to predict drug metabolite exposure: desipramine exposure in cytochrome P4502D6 extensive and poor metabolizers following administration of imipramine. *Drug Metab. Dispos.* **44**, 1569–1578 (2016).
6. Nguyen, H.Q., Kimoto, E., Callegari, E. & Obach, R.S. Mechanistic modeling to predict midazolam metabolite exposure from in vitro data. *Drug Metab. Dispos.* **44**, 781–791 (2016).
7. Nguyen, H.Q., Lin, J., Kimoto, E., Callegari, E., Tse, S. & Obach, R.S. Prediction of losartan-active carboxylic acid metabolite exposure following losartan administration using static and physiologically based pharmacokinetic models. *J. Pharm. Sci.* **106**, 2758–2770 (2017).
8. Obach, R.S. *et al*. Estimation of circulating drug metabolite exposure in human using in vitro data and physiologically based pharmacokinetic modeling: example of a high metabolite/parent drug ratio. *Drug Metab. Dispos.* **46**, 89–99 (2018).
9. Houston, J.B. Drug metabolite kinetics. *Pharmacol. Ther.* **15**, 521–552 (1981).
10. Shitara, Y., Horie, T. & Sugiyama, Y. Transporters as a determinant of drug clearance and tissue distribution. *Eur. J. Pharm. Sci.* **27**, 425–446 (2006).
11. Paine, S.W., Menochet, K., Denton, R., McGinnity, D.F. & Riley, R.J. Prediction of human renal clearance from preclinical species for a diverse set of drugs that exhibit both active secretion and net reabsorption. *Drug Metab. Dispos.* **39**, 1008–1013 (2011).
12. Mathialagan, S., Piotrowski, M.A., Tess, D.A., Feng, B., Litchfield, J. & Varma, M.V. Quantitative prediction of human renal clearance and drug-drug interactions of organic anion transporter substrates using in vitro transport data: a relative activity factor approach. *Drug Metab. Dispos.* **45**, 409–417 (2017).
13. Scotcher, D., Jones, C., Posada, M., Rostami-Hodjegan, A. & Galetin, A. Key to opening kidney for in vitro–in vivo extrapolation entrance in health and disease: part I: in vitro systems and physiological data. *AAPS J.* **18**, 1067–1081 (2016).
14. Pang, K.S. & Rowland, M. Hepatic clearance of drugs. I. Theoretical considerations of a "well-stirred" model and a "parallel tube" model. Influence of hepatic blood flow, plasma and blood cell binding, and the hepatocellular enzymatic activity on hepatic drug clearance. *J. Pharmacokinet. Biopharm.* **5**, 625–653 (1977).
15. Watanabe, T., Kusuhara, H., Maeda, K., Shitara, Y. & Sugiyama, Y. Physiologically based pharmacokinetic modeling to predict transporter-mediated clearance and distribution of pravastatin in humans. *J. Pharmacol. Exp. Ther.* **328**, 652–662 (2009).
16. Varma, M.V., Steyn, S.J., Allerton, C. & El-Kattan, A.F. Predicting clearance mechanism in drug discovery: extended clearance classification system (ECCS). *Pharm. Res.* **32**, 3785–3802 (2015).
17. Shitara, Y., Horie, T. & Sugiyama, Y. Transporters as a determinant of drug clearance and tissue distribution. *Eur. J. Pharm. Sci.* **27**, 425–446 (2006).
18. Maeda, K. *et al*. Identification of the rate-determining process in the hepatic clearance of atorvastatin in a clinical cassette microdosing study. *Clin. Pharmacol. Ther.* **90**, 575–581 (2011).
19. Prueksaritanont, T. *et al*. Pitavastatin is a more sensitive and selective OATP1B clinical probe than rosuvastatin. *Br. J. Clin. Pharmacol.* **78**, 587–598 (2014).
20. Liu, L. & Pang, K.S. The roles of transporters and enzymes in hepatic drug processing. *Drug Metab. Dispos.* **33**, 1–9 (2005).
21. Varma, M.V., Pang, K.S., Isoherranen, N. & Zhao, P. Dealing with the complex drug-drug interactions: towards mechanistic models. *Biopharm. Drug Dispos.* **36**, 71–92 (2015).
22. Mandema, J.W., Tuk, B., Van Steveninck, A.L., Breimer, D.D., Cohen, A.F. & Danhof, M. Pharmacokinetic-pharmacodynamic modeling of the central nervous system effects of midazolam and its main metabolite α-hydroxymidazolam in healthy volunteers. *Clin. Pharmacol. Ther.* **51**, 715–728 (1992).
23. Kupferschmidt, H.H.T., Ha, H.R., Ziegler, W.H., Meier, P.J. & Kraehenbuehl, S. Interaction between grapefruit juice and midazolam in humans. *Clin. Pharmacol. Ther.* **58**, 20–28 (1995).
24. Backman, J.T., Kivisto, K.T., Olkkolu, K.T. & Neuvonen, P.J. The area under the plasma concentration-time curve for oral midazolam is 400-fold larger during treatment with itraconazole than with rifampicin. *Eur. J. Clin. Pharmacol.* **54**, 53–58 (1998).
25. Eap, C.B. *et al*. Pharmacokinetics of midazolam in CYP3A4- and CYP3A5-genotyped subjects. *Eur. J. Clin. Pharmacol.* **60**, 231–236 (2004).
26. Link, B. *et al*. Pharmacokinetics of intravenous and oral midazolam in plasma and saliva in humans: usefulness of saliva as matrix for CYP3A phenotyping. *Br. J. Clin. Pharmacol.* **66**, 473–484 (2008).
27. Abernethy, D.R., Divoll, M., Greenblatt, D.J., Harmatz, J.S. & Shader, R.I. Absolute bioavailability of imipramine: influence of food. *Psychopharmacology* **83**, 104–106 (1984).
28. Sutfin, T.A., DeVane, C.L. & Jusko, W.J. The analysis and disposition of imipramine and its active metabolites in man. *Psychopharmacology* **82**, 310–317 (1984).
29. Brøsen, K., Otton, S.V. & Gram, L.F. Imipramine demethylation and hydroxylation: impact of the sparteine oxidation phenotype. *Clin. Pharmacol. Ther.* **40**, 543–549 (1986).
30. Wells, B.G. *et al*. The effect of ranitidine and cimetidine on imipramine disposition. *Eur. J. Clin. Pharmacol.* **31**, 285–290 (1986).
31. Bergstrom, R.F., Peyton, A.L. & Lemberger, L. Quantification and mechanism of the fluoxetine and tricyclic antidepressant interaction. *Clin. Pharmacol. Ther.* **51**, 239–248 (1992).
32. Callaghan, J.T., Cerimele, B.J., Kassahun, K.J., Nyhart, E.H. Jr, Hoyes-Beehler, P.J. & Kondraske, G.V. Olanzapine: interaction study with imipramine. *J. Clin. Pharmacol.* **37**, 971–978 (1997).
33. Kurtz, D.L., Bergstrom, R.F., Goldberg, M.J. & Cerimele, B.J. The effect of sertraline on the pharmacokinetics of desipramine and imipramine. *Clin. Pharmacol. Ther.* **62**, 145–156 (1997).
34. Albers, L.J. *et al*. Effect of venlafaxine on imipramine metabolism. *Psychiatry Res.* **96**, 235–243 (2000).
35. Sawant-Basak, A. *et al*. Metabolism of a serotonin-4 receptor partial agonist 4-{4-[4-tetrahydrofuran-3-yloxy)-benzo[d]isoxazol-3-yloxymethyl]-piperidin-1-ylmethyl}-tetrahydropyran-4-ol (TBPT): identification of an unusual pharmacologically active cyclized oxazolidine metabolite in human. *J. Pharm. Sci.* **102**, 3277–3293 (2012).
36. Lo, M.W., Goldberg, M.R., McCrea, J.B., Lu, H., Furtek, C.I. & Bjornsson, T.D. Pharmacokinetics of losartan, an angiotensin II receptor antagonist, and its active metabolite EXP3174 in humans. *Clin. Pharmacol. Ther.* **58**, 641–649 (1995).
37. Bienert, A. *et al*. Bioequivalence study of two losartan formulations administered orally in healthy male volunteers. *Arzneimittelforschung* **56**, 723–728 (2006).
38. Fischer, T.L. *et al*. Evaluation of potential losartan-phenytoin drug interactions in healthy volunteers. *Clin. Pharmacol. Ther.* **72**, 238–246 (2002).
39. Ohtawa, M., Takayama, F., Saitoh, K., Yoshinaga, T. & Nakashima, M. Pharmacokinetics and biochemical efficacy after single and multiple oral administration of losartan, an orally active nonpeptide angiotensin II receptor antagonist, in humans. *Br. J. Clin. Pharmacol.* **35**, 290–297 (1993).
40. Khandave, S.S., Sawant, S.V., Sahane, R.V., Murthi, V., Dhanure, S.S. & Surve, P.G. Bioequivalence study of two losartan tablet formulations with special emphasis on cardiac safety. *Int. J. Clin. Pharmacol. Ther.* **50**, 349–359 (2012).
41. Yasar, Ü. *et al*. Pharmacokinetics of losartan and its metabolite E-3174 in relation to the CYP2C9 genotype. *Clin. Pharmacol. Ther.* **71**, 89–98 (2002).
42. Walker, G.S., Bauman, J.N., Ryder, T.F., Smith, E.B., Spracklin, D.K. & Obach, R.S. Biosynthesis of drug metabolites and quantitation using NMR spectroscopy for use in pharmacologic and drug metabolism studies. *Drug Metab. Dispos.* **42**, 1627–1639 (2014).
43. Zhu, B., Bush, D., Doss, G.A., Vincent, S., Franklin, R.B. & Xu, S. Characterization of 1'-hydroxymidazolam glucuronidationin human liver microsomes. *Drug Metab. Dispos.* **26**, 331–338 (2008).
44. Zhu, B., Bush, D., Doss, G.A., Vincent, S., Franklin, R.B. & Xu, S. Characterization of 1'-hydroxymidazolam glucuronidation in human liver microsomes. *Drug Metab. Dispos.* **26**, 331–338 (2008).
45. Skjelbo, E., Brøsen, K., Hallas, J. & Gram, L.F. The mephenytoin oxidation polymorphism is partially responsible for the N-demethylation of imipramine. *Clin. Pharmacol. Ther.* **49**, 18–23 (1991).
46. Koyama, E. *et al*. Metabolic disposition of imipramine in oriental subjects: relation to metoprolol alphahydroxylation and S-mephenytoin 49-hydroxylation phenotypes. *J. Pharmacol. Exp. Ther.* **271**, 860–867 (1994).
47. Lo, M.W., Goldberg, M.R., McCrea, J.B., Lu, H., Furtek, C.I. & Bjornsson, T.D. Pharmacokinetics of losartan, an angiotensin II receptor antagonist, and its active metabolite EXP3174 in humans. *Clin. Pharmacol. Ther.* **58**, 641–649 (1995).
48. Cozaar Package Insert. <https://www.medicines.org.uk/emc/product/1576/pil>.